ChemPubSoc Europe

DOI: 10.1002/chem.201503732

CHEMISTRY
A European Journal
Full Paper

Synthesis Design

Azaphilic versus Carbophilic Coupling at C=N Bonds: Key Steps in Titanium-Assisted Multicomponent Reactions

Torsten Roth,[a] Hubert Wadepohl,[a] Eric Clot,*[b] and Lutz H. Gade*[a]

In memoriam Peter Hofmann

Abstract: Consecutive C- and N-arylation of N-heterocyclic nitriles is mediated by titanium(IV) alkoxides. The carbo- and azaphilic arylation step may be separated by choosing the order in which the two equivalents of aryl transfer reagent are added. In the course of this transformation, the ancillary N-heterocycle acts as both a directing anchor group and electron reservoir. In the selectivity-determining step, the selectivity is governed by a choice between (direct) C- and Ti-arylation; the latter opens up a reaction pathway that allows further migration to the nitrogen atom. The isolation of metal-containing aggregates from the reaction mixture and computational studies gave insights into the reaction mechanism. Subsequently, a multicomponent one-pot protocol was devised to rapidly access complex quaternary carbon centers.

Introduction

In general, the reaction of nucleophilic alkyl or aryl metal compounds with C=N groups yields the corresponding C-alkylated or -arylated products.[1] Nevertheless, a number of cases are known in which this "normal" regioselectivity is suppressed in favor of an azaphilic addition ("umpolung").[2,3] An early example of this unexpected addition mode was reported by Kagan and Fiaud in 1971 for the reaction of Grignard reagents with α-iminoesters,[4a] and since then has been expanded into a viable route to α-amino esters.[4,5] Additionally, imino groups in special electronic environments, such as cyclopentadieneimines, have been found to follow similar reactive patterns.[6]

The observed azaphilic regioselectivity has been attributed, among other things, to the potentially chelating coordination of a Lewis acidic metal cation (Mg^{2+} for Grignard reagents) by the substrate; this results in a conformation that favors N-addition as well as polarization of the C=N bond due to the electron-withdrawing properties of the adjacent functional group (in α-iminoesters). Another qualitative rationale refers to the similarity of this structural motif in α-iminoesters to the well-known nucleophilic addition to vinylogous systems. Unfortunately, there is limited insight into this pattern of reactivity available from studies focusing on the underlying organometallic chemistry, experimental mechanistic work, or computational modeling.

Herein, we demonstrate how the polarization and orientation of metal-coordinated ketimides may influence the regiochemistry of Grignard additions to CN multiple bonds. The focal point in the assembly is tetravalent titanium, which effects the fixation and orientation of the substrates, and thus controls the relative approach of key reagents.[7,8] The presence of additional functional groups that act as ligating units may significantly alter the preferred coordination mode of the ketimide and, as will be demonstrated, the observed pattern of reactivity (Figure 1).

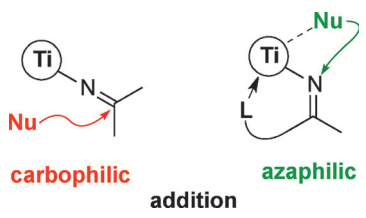

Figure 1. Schematic representation of opposing patterns of reactivity.

[a] T. Roth, Prof. H. Wadepohl, Prof. L. H. Gade
Anorganisch-Chemisches Institut, Universität Heidelberg
Im Neuenheimer Feld 270, 69120 Heidelberg (Germany)
E-mail: lutz.gade@uni-heidelberg.de

[b] Dr. E. Clot
Institut Charles Gerhardt, CNRS 5253, cc 1501
Université de Montpellier, Place Eugène Bataillon
34000 Montpellier (France)
E-mail: eric.clot@umontpellier.fr

Supporting information for this article is available on the WWW under http://dx.doi.org/10.1002/chem.201503732. It contains preparative methods, spectroscopic data, and full computational details.

Results and Discussion

Consecutive carbo- and azaphilic addition of Grignard reagents to N-heterocyclic nitriles

Ketimide compounds have been generated in situ by the group of de Meijere and others through the reaction of Grignard reagents with various nitriles, including heterocyclic derivatives (3- and 4-pyridine-, 2-thiophene-, 2-furan-carbonitrile, etc.) to yield the corresponding trityl amine products.[9] The starting point for our study was the observation that the reaction of 2-pyridine carbonitrile with aryl Grignard reagents under the same conditions as those described by de Meijere et al., and subsequent hydrolytic workup gave N-arylated amines, and thus, the products of azaphilic addition (Scheme 1).

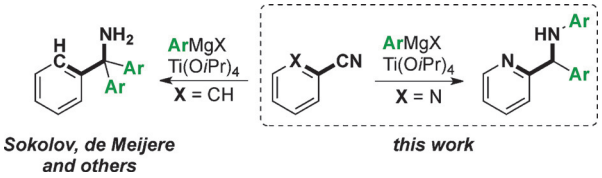

Scheme 1. Regioselection due to chelation control.

We hypothesized that this unexpected regioselectivity was due to chelation control by the pyridyl ring, which generated reactive intermediates coordinated to the metal center that, in turn, could act as key species in metal-complex-induced, multicomponent one-pot reactions. The critical role played by the N-heterocyclic ring within the substrate for this reactive pattern was supported by control reactions (see the Supporting Information) as well as the isolation of a series of other *N*-aryl benzhydryl amines by the same titanium-mediated route (Table 1).

Significantly, we were able to separate the carbo- and azaphilic arylation steps, and thus, selectively introduce different aryl substituents, by choosing the order in which the two equivalents of Grignard reagent were added (Table 2): the first equivalent of Grignard reagent cleanly added to the nitrile carbon, whereas the second addition only took place in the presence of $[Ti(OiPr)_4]$ and occurred at the nitrogen atom. The reaction is not limited to Grignard reagents nor to the presence of magnesium salts, since the corresponding lithium compounds are equally applicable in this transformation (compounds **2j** and **2k**).

Isolation and structural characterization of a magnesium imide and a magnesium–titanium heterobimetallic imido complex

To obtain mechanistic insights into this intriguing transformation, we aimed to isolate crystalline products of the individual reaction steps that might represent or be related to reaction intermediates. First, Grignard addition onto the nitrile moiety was investigated for the addition of 4-fluorophenylmagnesium bromide to 2-pyridine carbonitrile in THF at room temperature.

Table 1. Variation of the N-heterocyclic unit.

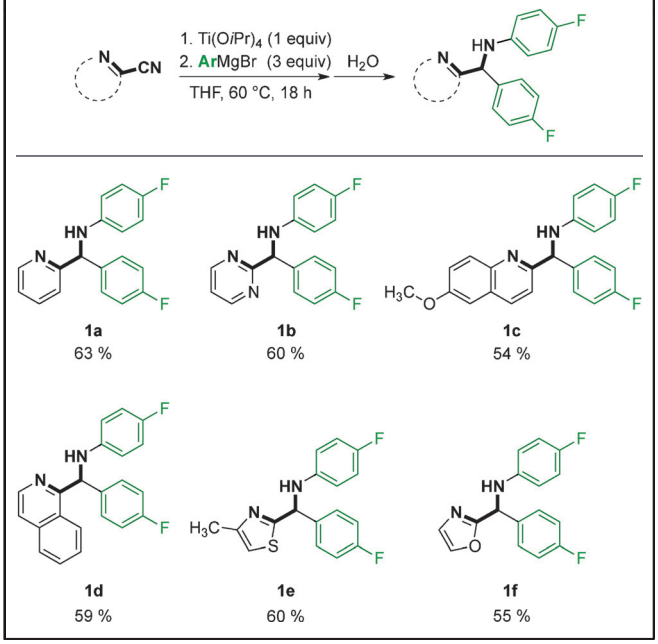

Notably, and crucially, for the selectivity of this transformation, the magnesium imide generated in this reaction step is not susceptible to further reaction with excess Grignard reagent.

A single-crystal X-ray structure analysis of the ketimido–magnesium compound **3** established the structural details of an octameric aggregate (Figure 2), in which the 2-pyridylimido unit acts as a chelating ligand for magnesium.[10]

This leads to a bent structure of the metal–ketimido fragment, which exposes the imido-*N* atom that acts as a bridging ligating unit to a neighboring magnesium center. The observed reactivity in subsequent transformations indicates at least partial fragmentation of the octamer under the reaction conditions (Figure 2).

The subsequent reaction step, transmetalation with the titanium reagent, was studied by reacting **3** with $[Ti(OiPr)_4]$ and $[TiBr(OiPr)_3]$ (Scheme 2). In both cases, in situ ^1H and ^{13}C NMR spectroscopy as well as mass spectrometry results indicated the formation of a mixture of molecular species that defied characterization. However, with $[TiBr(OiPr)_3]$, we isolated a crystalline reaction product that could be characterized, inter alia, by XRD (Figure 3). The product was a Ti/Mg heterodinuclear complex **4**, in which the Ti atom is coordinated by a bromide ligand, two remaining isopropoxido units and two chelating 2-pyridylimido units, one of which bridges the titanium and magnesium centers. The coordination sphere of magnesium is completed by a halogenido ligand and a coordinated THF molecule.

The 2-pyridylimides act as bidentate chelates, and thus, feature bent ketimido–metal units. This form of ligation, which is significant for the subsequent transformations discussed below, should be seen in comparison with the large number of structurally characterized ketimides of the early transition metals, most of which adopt near-linear C=N–metal arrangements.[11]

Table 2. Variation of the alkyl/aryl organometallics. The molecular structure of product **2i** is shown in the bottom-right corner. Thermal ellipsoids are set at the 50% probability level.

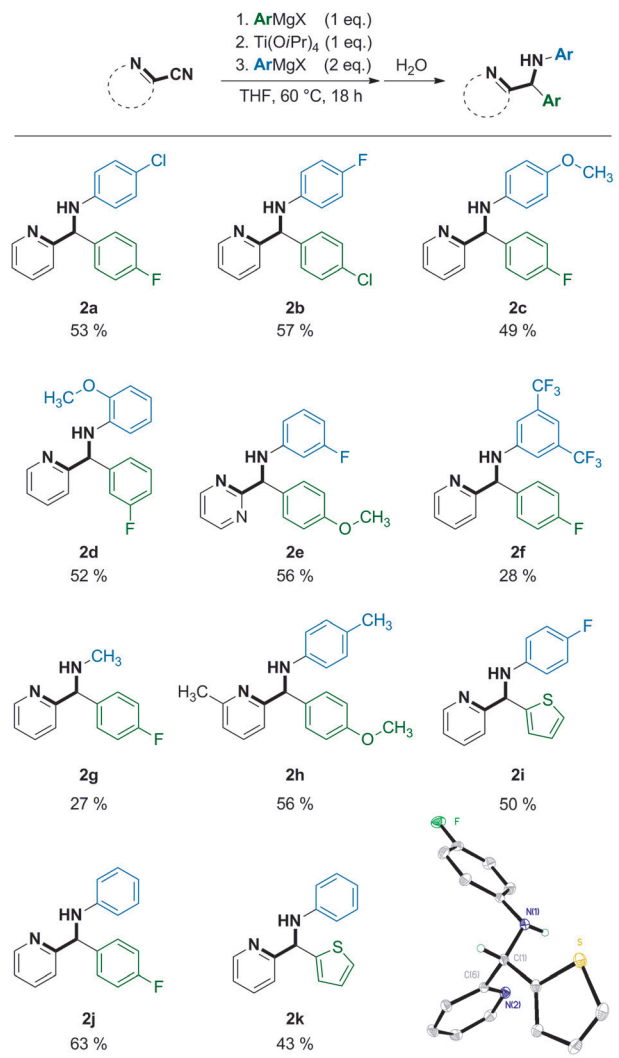

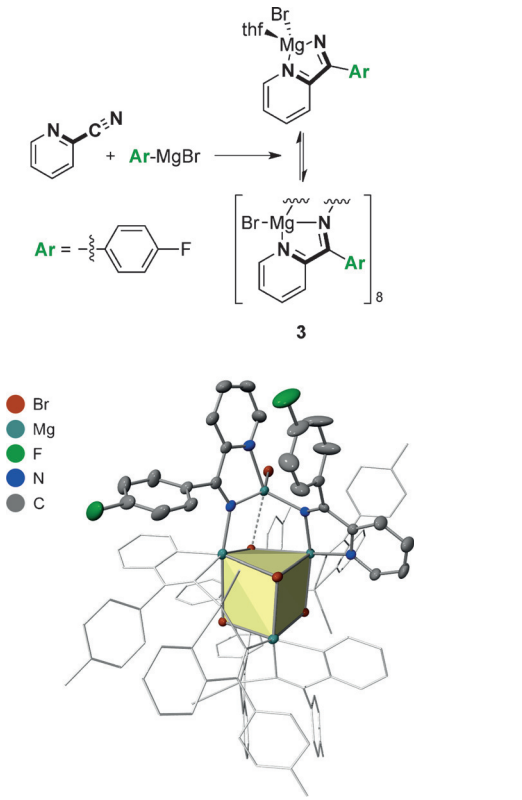

Figure 2. Top: In situ formation of oligomeric Mg–ketimido clusters. Bottom: Octameric Mg–ketimide cluster **3** arranged around a central Mg_4Br_4 core. Thermal ellipsoids are set at the 50% probability level. Hydrogen atoms and cocrystallized solvent molecules have been omitted for clarity. The central cube has been highlighted. For selected bond lengths and angles, see the Supporting Information.

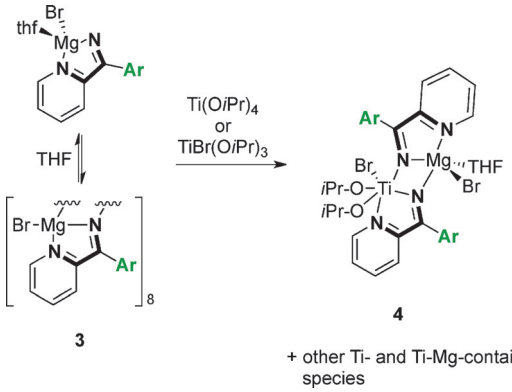

Scheme 2. In situ formation of labile titanium- and magnesium-containing heterometallic species.

The following key reaction step of the transformation, leading to the reaction products represented in Table 1 and 2, involves attack of the second Grignard reagent and determines whether carbo- or azaphilic coupling is favored. Given the complex equilibria of aggregates encountered in this type of chemistry, which precludes in situ characterization by spectroscopic means as well as systematic kinetic studies, additional insight had to be drawn from a computational study (PBE0 calculations) by employing an appropriately chosen model system (see the Supporting Information for computational details).

DFT modeling of aza- versus carbophilic coupling to C=N bonds

In the first stage, the simplest product of transmetalation between **3** and $Ti(OiPr)_4$ (or $TiBr(OiPr)_3$) was considered. This complex features three alkoxy ligands (herein modeled by OMe) and one ketimide $N_\alpha{=}C_\beta(Py)(Ar)^-$ (Py = 2-pyridine; Ar = para-fluorophenyl) with either coordination of the pyridine substituent (**A-cyc**) or lack of pyridine coordination (**A**). The two optimized geometries are shown in Figure 4 and **A-cyc** is computed to be more stable than **A** by $\Delta G = -3$ kcal mol^{-1}. The geometry of **A** has a pseudo-C_{3v} geometry with three almost identical Ti–O bonds (1.784, 1.788, and 1.802 Å) and a significantly

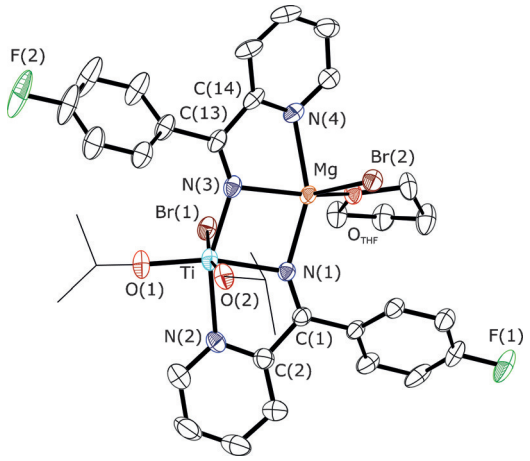

Figure 3. Isolated heterometallic titanium- and magnesium-containing adduct **4**. Thermal ellipsoids are set at the 50% probability level. Hydrogen atoms and cocrystallized solvent molecules have been omitted for clarity. For selected bond lengths and angles, see the Supporting Information.

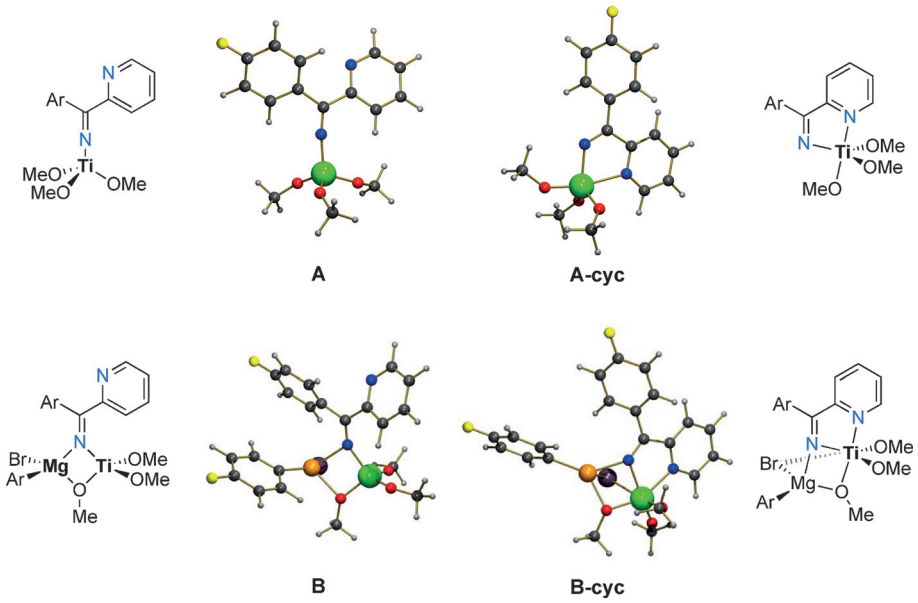

Figure 4. Computed structures of the Ti complex fragments **A** and **A-cyc** and the Ti–Mg heterodinuclear model complexes **B** and **B-cyc**. The optimized geometries are available in a single xyz file (Geom.xyz) in the Supporting Information. Color code: green = Ti, purple = Br, orange = Mg, yellow = F, red = O, blue = N, dark gray = C, light gray = H.

shortened Ti–N_α distance of 1.865 Å, which is indicative of some double bond (i.e., azavinylidene) character.[12] Upon pyridine coordination in **A-cyc**, the geometry becomes a trigonal bipyramidal with the apical pyridine unit and a methoxy ligand. The Ti–N_α bond is significantly elongated at 1.988 Å, whereas the N_α=C_β distance remains unchanged (1.269 Å, **A**; 1.268 Å, **A-cyc**).

A natural bonding orbital (NBO) analysis of the electronic structure of **A** and **A-cyc** highlighted significantly different electronic properties of the N_α=C_β bond in **A** and **A-cyc**. The natural localized molecular orbital (NLMO) for the π bond between N_α and C_β is delocalized on the Ti center with overall weights of 2.7, 57.1, and 37.1% on Ti, N_α, and C_β, respectively. For the same NLMO, the respective weights are 1.9, 52.2, and 42.1% in **A-cyc**. This indicates that the N_α=C_β bond is more polarized toward C_β in **A-cyc** than in **A**. Therefore, the carbon atom is more electron-rich in **A-cyc** than that in **A**, and thus, less prone to attack by a nucleophile. This is also reflected in the natural population analysis (NPA) charge for C_β, which is more positive in **A** than that in **A-cyc** (0.286 vs. 0.215). In other words, the binding of pyridine lowers the intrinsic reactivity of C_β towards a nucleophilic reagent.

Coordination of Mg(Br)(Ar) (Ar = parafluorophenyl) to either **A** or **A-cyc** is exergonic by $\Delta G = -7.7$ and -17.5 kcal mol^{-1}, respectively. The geometries of adducts **B** and **B-cyc** are shown in Figure 4. In adduct **B**, the Mg cation is bridging between N_α and one methoxy ligand (N_α···Mg = 2.286 Å and Mg···O = 2.122 Å). The Ti–N_α–C_β linkage deviates from linearity in adduct **B** with Ti-N_α-C_β = 148°. The N_α=C_β bond is slightly elongated (1.284 Å) and the NLMO associated with the π bond is more strongly polarized toward N_α in adduct **B** than that in the mononuclear reference system **A** (60.1% N_α, 34.2% C_β, 2.9% Ti; charge on C_β in **B**: 0.334). Coordination of Mg(Br)(Ar) has increased the reactivity of C_β toward a nucleophile. In **B-cyc**, the Mg cation is bridging between N_α and the apical methoxy ligand (Mg···N_α = 2.089 Å, Mg···O = 2.027 Å).

The initial trigonal bipyramidal geometry of **A-cyc** is altered upon coordination of MgBr(Ar) to a pseudo-octahedral geometry with creation of a Ti···Br interaction (2.842 Å); thus explaining the larger binding energy. As in the case of **B**, the formation of the adduct increases the reactivity of C_β toward a nucleophile. The geometry of **B-cyc** is qualitatively similar to that observed for the isolated hetereobimetallic adduct (Figure 3).

The transition state, **TS-B-C** (Figure 5), corresponding to the arylation of C_β in **B** has been located on the potential energy surface with $\Delta G^{\ddagger} = 25.9$ kcal mol^{-1}. In **TS-B-C**, the forming C···C bond length is 2.386 Å, whereas the N_α=C_β bond is elongated to 1.333 Å and the Mg–Ar bond length increases from 2.110 Å in **B** to a value of 2.185 Å in **TS-B-C**. The C-arylation is exergonic with $\Delta G = -12.9$ kcal mol^{-1} and, in the product of C-arylation, **C** (Figure 5), the Mg cation is bridging N_α (2.105 Å) and one methoxy unit (1.976 Å).

In the transition state **TS-B-C-cyc** (Figure 5), in which pyridine is coordinated to Ti, the forming C···C bond has an intera-

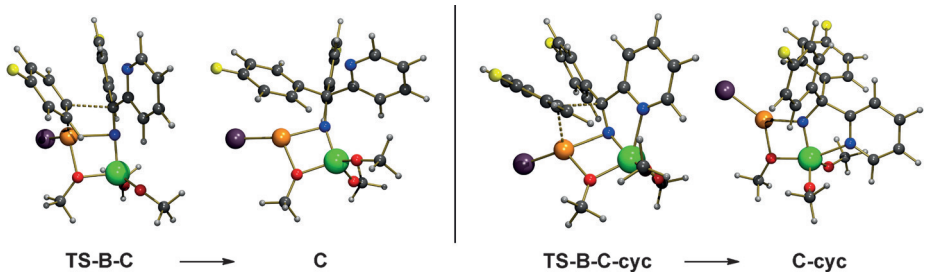

Figure 5. Optimized geometries of the various extrema located along the pathway for direct C-arylation without (left) or with (right) pyridine coordination. The optimized geometries are available in a single xyz file (Geom.xyz) in the Supporting Information. Color code: green = Ti, purple = Br, orange = Mg, yellow = F, red = O, blue = N, dark gray = C, light gray = H.

tomic distance similar to that observed in **TS-B-C** (2.380 Å). However, the N_α=C_β bond is less elongated (1.317 Å) and the breaking Mg···Ar bond is longer (2.290 Å) in **TS-B-C-cyc**. This is in agreement with a greater reactivity of C_β toward nucleophilic attack in **B** than that in **B-cyc**.

As a matter of fact, the activation barrier associated with **TS-B-C-cyc** is greater ($\Delta G^{\neq}$ = 30.4 kcal mol^{-1}) than that for **TS-B-C** ($\Delta G^{\neq}$ = 25.9 kcal mol^{-1}). There is thus a significant decrease in the C-arylation reactivity upon coordination of pyridine.

From **B** or **B-cyc**, no transition-state structures associated with direct transfer of Ar from Mg to N_α could be located on the potential energy surface. However, in both cases, a transition-state structure associated with Ar transfer from Mg to Ti could be located. In the case of **TS-B-D** (Figure 6), when pyridine is not coordinated, the activation barrier is low, $\Delta G^{\neq}$ = 8.9 kcal mol^{-1}, and the transformation is endergonic, ΔG = 6.9 kcal mol^{-1} for **D** relative to **B**. The product of the reaction, **D**, features an aromatic ring bridging Mg and Ti (Mg···C = 2.247 Å and Ti···C = 2.353 Å, see Figure 6).

With pyridine coordinated, the activation barrier associated with **TS-B-D-cyc** is slightly lower ($\Delta G^{\neq}$ = 4.8 kcal mol^{-1}) and the transformation is still endergonic, with **D-cyc** lying at ΔG = 2.8 kcal mol^{-1} above **B-cyc**. Here again, the transferring aromatic ring is bridging Mg and Ti in the product **D-cyc** (Mg···C = 2.366 Å and Ti···C = 2.317 Å, see Figure 6).

From intermediate **D**, N-arylation is effective through **TS-D-E** with an activation barrier of $\Delta G^{\neq}$ = 20.8 kcal mol^{-1} and leads to the N-arylated product **E** with ΔG = −12.0 kcal mol^{-1}. In **TS-D-E**, the migrating aryl group is bridging the Ti–N_α bond (Ti···C = 2.190 Å and N_a···C = 1.784 Å) and the N_α=C_β bond is elongated to 1.342 Å.

The product of the reaction, **E**, features a ketimine moiety, N_α(Ar)=C_β(Py)(Ar), in which the Ti center interacts both with the N_α–C_β (Ti···N_α = 2.081 Å and Ti···C_β = 2.112 Å) and C_β–Ar bonds (Ti···Ar = 2.482 Å), whereas the Mg cation interacts with N_α (2149 Å) and two methoxy groups.

Interestingly, the energetics associated with the corresponding N-arylation from **D-cyc** is similar, with **TS-D-E-cyc** lying at $\Delta G^{\neq}$ = 21.0 kcal mol^{-1} above **D-cyc** and **E-cyc** lying at ΔG = −13.1 kcal mol^{-1} below **D-cyc**. However, this energetic similarity does not translate into similar geometric parameters. The migrating aromatic ring is further away from both Ti (Ti···C = 2.463 Å) and N_α (N_α···C = 1.930 Å) in **TS-D-E-cyc** compared with **TS-D-E**. Only the N_α=C_β bond exhibits a similar lengthening (1.344 Å). Because of pyridine coordination, the ketimine moiety, N_α(Ar)=C_β(Py)(Ar), in product **E-cyc** only interacts with Ti through the N_α=C_β bond (Ti···N_α = 2.057 Å and Ti···C_β = 2.272 Å). The Mg cation is bridging N_α (Mg···N_α = 2.088 Å) and one methoxy group.

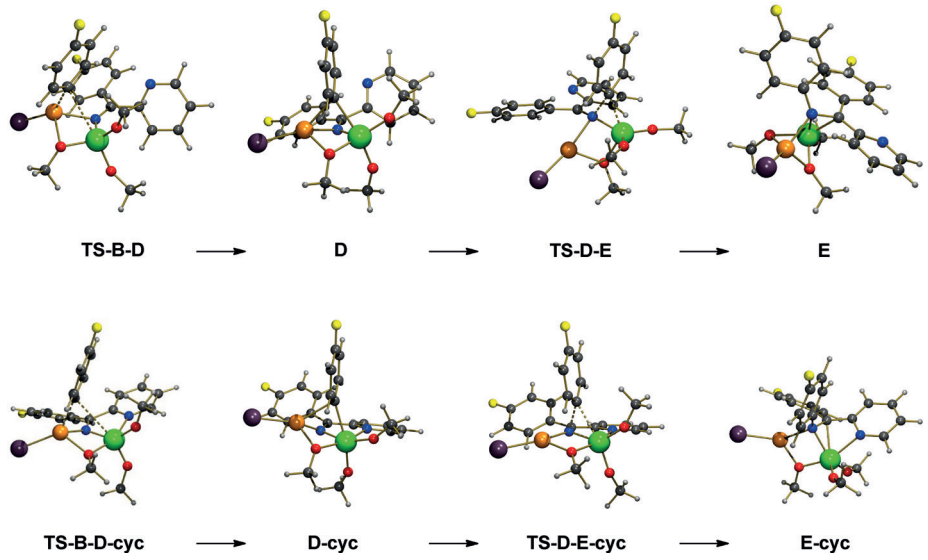

Figure 6. Optimized geometries of the various extrema located along the pathway for N-arylation without (top) or with (bottom) pyridine coordination. The optimized geometries are available in a single xyz file (Geom.xyz) in the Supporting Information. Color code: green = Ti, purple = Br, orange = Mg, yellow = F, red = O, blue = N, dark gray = C, light gray = H.

In Figure 7a, a comparison between the pathways for C- and N-arylation when pyridine is not coordinated is shown (decoord pathway). The C-arylation pathway is preferred both kinetically and thermodynamically. Although aromatic ring transfer is intrinsically easier from Ti to N_α than it is from Mg to C_β, the energy needed to transfer the aromatic ring from Mg to Ti overall destabilizes the N-arylation pathway. A comparison between the pathways for C- and N-arylation when pyridine is coordinated (metallacycle pathway) is shown in Figure 7b . Although the product of C-arylation is pre-

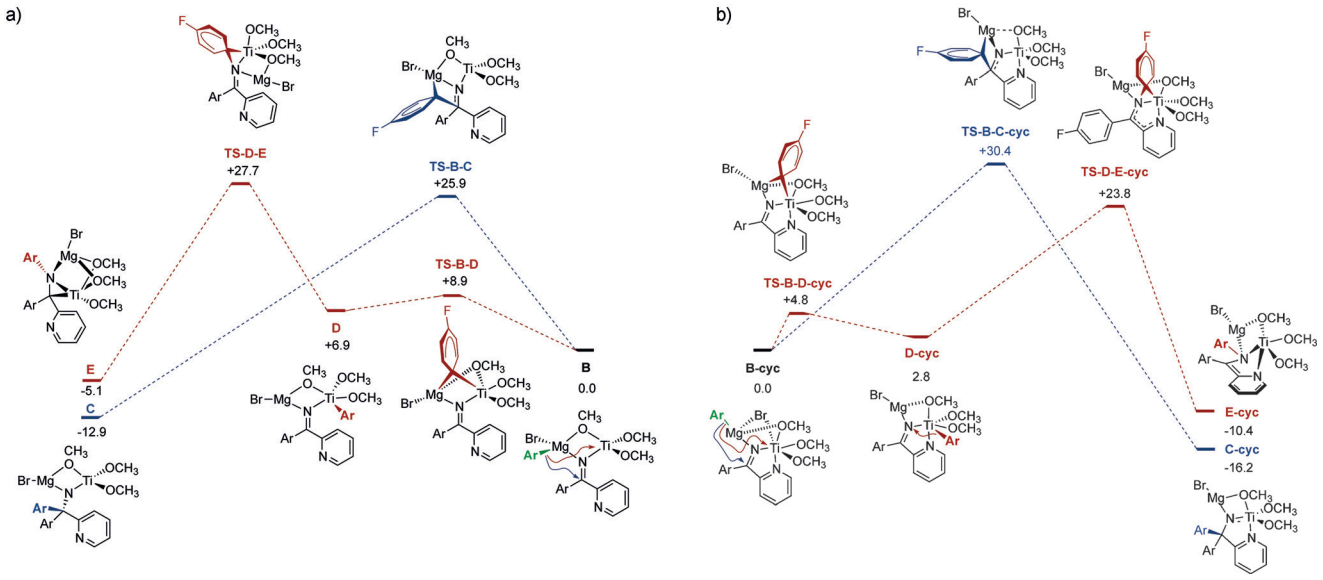

Figure 7. Comparison between the pathways for C- and N-arylation without (a) and with pyridine coordination (b). Gibbs free energy values are expressed in kcal mol^{-1} at 333 K relative to **B** (path a) or to **B-cyc** (path b); **B-cyc** is 12.7 kcal mol^{-1} more stable than **B**.

ferred thermodynamically, the formation of the N-arylated product is preferred kinetically.

The kinetic preference for the N-arylation pathway is the result of two cooperative effects. As already explained, pyridine coordination reduces the intrinsic reactivity of C_β toward direct reaction with a nucleophile. This leads to an increase in the energy of **TS-B-C-cyc** with respect to **B-cyc**, compared with the energy of **TS-B-C** with respect to **B**. In addition, aromatic ring transfer from Mg to Ti is slightly favored when pyridine is coordinated (by ca. 4 kcal mol^{-1}; compare **TS-B-D-cyc** in Figure 7b with **TS-B-D** in Figure 7a).

Consequently, the transition state of the rate-determining step for the C-arylation pathway is destabilized, whereas that of the rate-determining step for N-arylation is stabilized when pyridine is coordinated. This eventually leads to inversion of the kinetically preferred pathway in favor of N-arylation when a substituent on the arylated ketimide can coordinate to titanium, as observed experimentally (Table 1). When such coordination is not possible, the expected C-arylation product will be obtained.

In summary, the proposed mechanism of the azaphilic C–N coupling has revealed that the initial idea of an umpolung, in which a nucleophile is added onto the more electronegative nitrogen, has to be revised. In fact, in the selectivity-determining step, the choice is not between N- and C-arylation, but between C- and Ti-arylation; the latter opens up a reaction pathway that allows further migration to the nitrogen atom.

The reaction product for the pathway involving azaphilic coupling, **E-cyc**, represents a local minimum on the free energy hypersurface, and may rearrange to a pyridyl-ligated titanaaziridine complex, **F-cyc**, as depicted in Scheme 3. Complex **F-cyc** is computed to be $\Delta G = -7.7$ kcal mol^{-1} more stable than **E-cyc**. It is therefore reasonable to assume that such a species represents a key intermediate for the subsequent conversions discussed below.

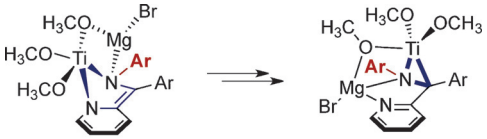

Scheme 3. Internal rearrangement of the titanium–enediamido species **E-cyc** to the corresponding energetically favorable chelated magnesium/titanaaziridine complex **F-cyc**. Gibbs free energy values (kcal mol^{-1}, 333 K) are expressed relative to **B-cyc**.

In recent work by Müller, Beckhaus and co-workers, aromatic aldimine and ketimine complexes of titanocene were studied to highlight the accessibility and close structural relationship of three- and five-membered titanacycles (Figure 8).[13a] A structurally related example was reported by Rosenthal et al.[13b] It was rationalized that steric factors determined the preferred coordination mode (titanaaziridine vs. 1-aza-2-titanacyclopent-4-ene species).[13]

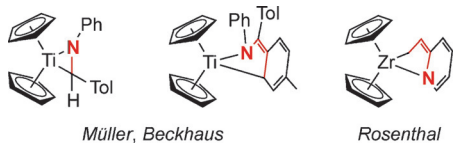

Figure 8. Structurally characterized titanaaziridine and azatitanacyclopentene complexes.

Development of multicomponent reactions based on sequential C- and N-arylation steps

A key insight of the computational study described above has been the likely formation of the titanaaziridine species **F-cyc**, which may thus be viewed as a key intermediate for subsequent reaction steps in the multicomponent transformations described herein. The reactivity of metallacyclic aziridines of the Group 4 metals has been studied previously by several research groups and has given rise to exciting examples of metal-induced transformations.[14] The most common pattern of reactivity involves the coupling of the metal-bonded carbon atom with various electrophilic reagents, including aldehydes or alkyl halides. This opened up the possibility of developing the one-pot formation of such species into multiple-component reactions for synthetic targets, in which quaternary carbon centers with four different substituents would be accessible in a chemoselective way.[15]

Initially, we examined the addition of a range of different electrophiles to the reaction mixture prior to hydrolytic workup.

Upon the addition of an excess of paraformaldehyde, the oxazolidines **5a**,**b** were isolated as the main products, depending on the electronic nature of the N-aryl substituent (Scheme 4). The oxazolidine is thought to be formed by a Mannich-type mechanism from an initial β-aminoalcohol intermediate.

Subsequently, the reactive potential of the titanaaziridine intermediate towards various alkyl halides was investigated. Both allyl and benzyl bromides afforded the corresponding trisubstituted amines (Scheme 5).

Remarkably, and in contrast to the reaction involving formaldehyde, which had to be added in the final step of the one-pot procedure, the halides were found to be inert under the reaction conditions chosen for the formation of the active titanium species, and therefore, could be added during the initial setup of the reaction, rendering this a true one-pot, multicomponent coupling.

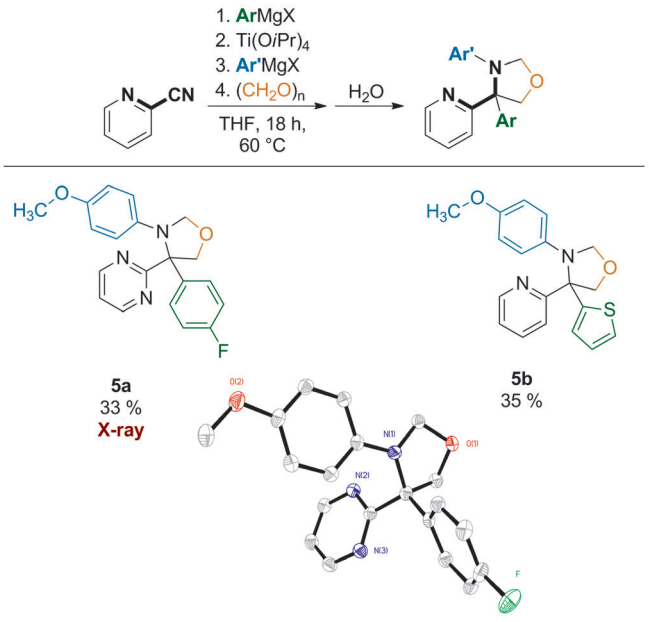

Scheme 4. In situ trapping of the intermediary titanium species with formaldehyde. Hydrogen atoms in the molecular structure of **5a** have been omitted for clarity; thermal ellipsoids are shown at the 50% probability level.

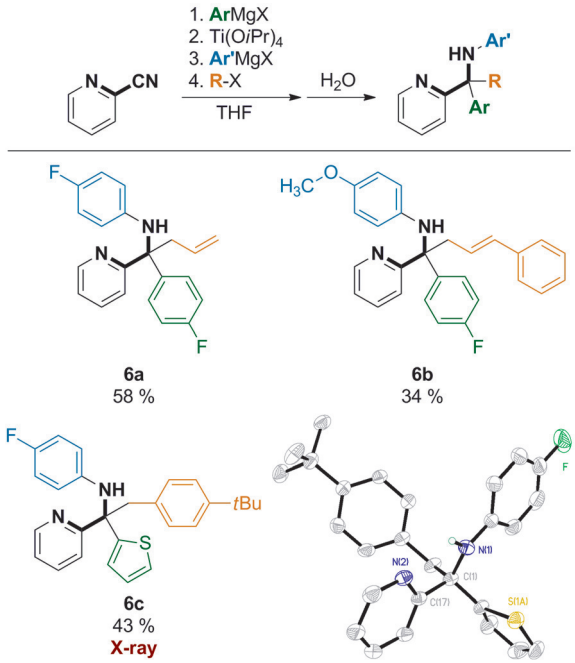

Scheme 5. In situ trapping of the intermediary titanium species with alkyl halides. The molecular structure of **6c** is shown in the bottom-right corner. Hydrogen atoms, except for N(1)–H have been omitted for clarity; thermal ellipsoids are shown at the 50% probability level.

Recently, Micalizio and co-workers reported the reaction of in situ generated azatitanacyclopropanes (generated from imines and the Sato reagent[16]) with allylic or allenylic alkoxides to yield homoallylic amines or dienes.[17a–d] This approach was used, inter alia, for the synthesis of complex natural products. Reacting allylic alkoxides with the titanium intermediate, we observed the formation of the corresponding homoallylic amines (Scheme 6).

Again, the allylic alkoxide could be added directly to the reaction mixture and did not interfere with the Ti–N aryl transfer. Using chiral allylic alkoxides as coupling partners, we obtained the corresponding enantioenriched reaction products, albeit with a slight erosion of chirality.[18] Chirality is thus transferred from an easily accessible chiral allylic alcohol to a metallacycle, thereby creating an enantioenriched quaternary carbon atom. The selectivity observed in this transformation is consistent with an empirical model based on a formal metallo-[3,3]-rearrangement.[17]

Finally, we exchanged the allylic alkoxides for allenylic alkoxides.[19] Instead of the expected diene-containing product, the 1,5-aminoalkohols **8a** and **8b** were isolated (Scheme 7). The results of a workup in D_2O (**8a**-d_1) suggest a reaction mechanism through 1,2-carbometalation of the terminal allene π bond, in contrast to the previously reported formal metallo-[3,3]-rearrangement.

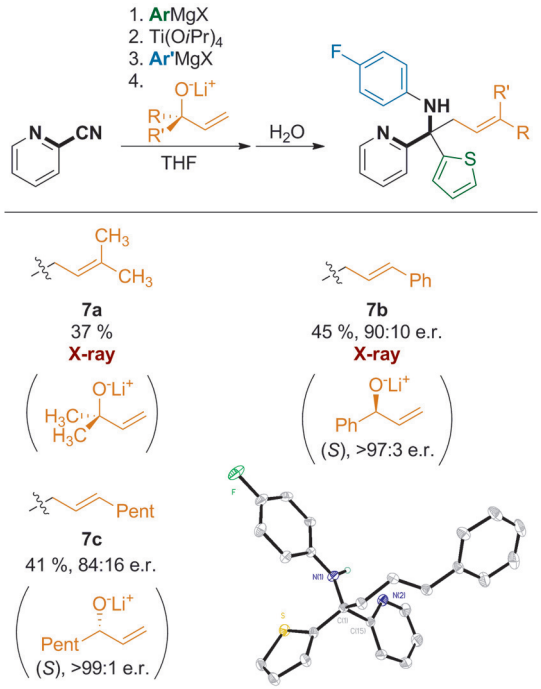

Scheme 6. Multicomponent reactions employing allylic alkoxides. The respective starting materials are given in brackets. The molecular structure of **7b** is shown in the bottom-right corner. Hydrogen atoms, except for N(1)–H, have been omitted for clarity; thermal ellipsoids are shown at the 50% probability level. A rationale for the observed *E* selectivity of these transformations based on an empirical model is depicted in the Supporting Information.

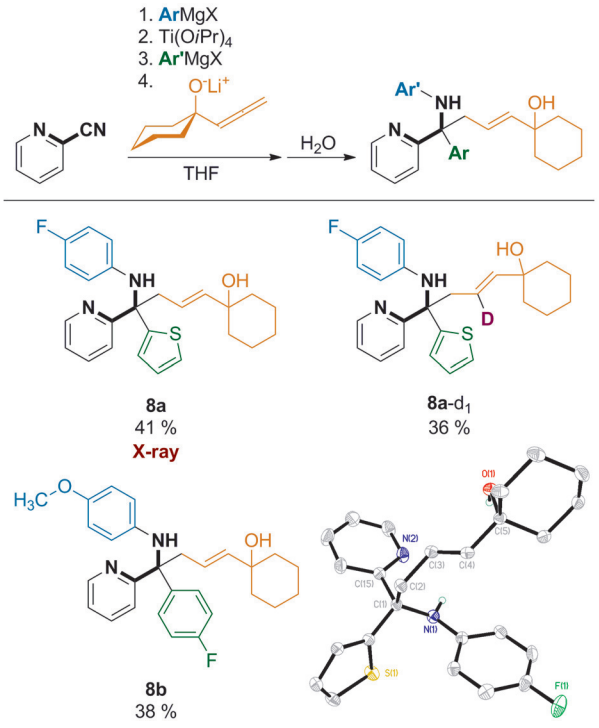

Scheme 7. A multicomponent reaction employing an allenylic alkoxide. The molecular structure of **8a** is shown in the bottom-right corner. Hydrogen atoms, except for N(1)–H and O(1)–H, have been omitted for clarity; thermal ellipsoids are shown at the 50% probability level.

Conclusion

We have developed a powerful new multicomponent strategy for the rapid convergent assembly of structural complexity starting from simple N-heterocyclic nitriles, Grignard reagents, and electrophilic coupling agents. Notably, this process relies on inexpensive, readily available starting materials, is highly modular, and yields environmentally benign and easily separable byproducts.

The range of products thus accessible comprises valuable nitrogen-containing heterocycles, enantioenriched quaternary carbon centers, and densely functionalized structural motifs of pharmaceutical and biomedical relevance, as exemplified by the class of cholesterylester transfer protein (CETP) inhibitors shown in Figure 9.[20,21]

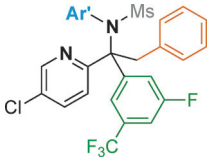

Figure 9. CETP inhibitors comprising an *N*-aryl tritylamine motif (Ms = mesyl).

Whereas the reaction products described herein are accessible through conventional approaches, namely, nucleophilic addition to diarylimines, these methods require multiple steps and tedious workup procedures.[22] The reaction mechanism of the unexpected azaphilic addition of nucleophiles to ketimide titanium complexes was explored by DFT methods, which revealed the formal umpolung of a C–N group as the key step toward reactive intermediary metallacycles (titanaziridines and azatitanacyclopentenes). A central role is attributed to the tethered nitrogen donor moiety, which serves as a precoordinating directing group and, in conjunction with an ancillary π system, as an electron reservoir.

Finally, the reactivity profile of the titanacyclic intermediates was assessed by four mechanistically distinct follow-up reactions, namely, by insertion reactions with a C=O function, by nucleophilic substitution of halogenated alkanes, by allylic alkoxides featuring a formal metallo-[3,3]-rearrangement, and by allenic alkoxides resulting in a 1,2-carbometalation reaction. Notably, these transformations show a high degree of regioselectivity, although the control of absolute stereochemistry in this process remains a challenge. Moreover, the step-economic concept presented in this work shows the great utility of Group 4 metals for mediating challenging C–C and C–N bond formations.

Acknowledgements

We gratefully acknowledge the award of a Ph.D. grant to T.R. from the Landesgraduiertenförderung (LGF Funding Program of the state of Baden-Württemberg) and the University of Heidelberg for generous funding.

Keywords: heterocycles · metallacycles · multicomponent reactions · synthetic methods · titanium

[1] For review articles, see: a) S. Kobayashi, Y. Mori, J. S. Fossey, M. M. Salter, *Chem. Rev.* **2011**, *111*, 2626 – 2704; b) G. K. Friestad, A. K. Mathies, *Tetrahedron* **2007**, *63*, 2541 – 2569; c) S. Kobayashi, H. Ishitani, *Chem. Rev.* **1999**, *99*, 1069 – 1094; d) R. Bloch, *Chem. Rev.* **1998**, *98*, 1407 – 1438; e) D. Enders, U. Reinhold, *Tetrahedron: Asymmetry* **1997**, *8*, 1895 – 1946.

[2] The term *umpolung* has been defined by Seebach as "any process by which donor and acceptor reactivity of an atom are interchanged": D. Seebach, *Angew. Chem. Int. Ed. Engl.* **1979**, *18*, 239 – 258; *Angew. Chem.* **1979**, *91*, 259 – 278. See also: a) J. J. Eisch, *J. Organomet. Chem.* **1995**, *500*, 101 – 115; b) H. R. Guan, *Curr. Org. Chem.* **2008**, *12*, 1406 – 1430.

[3] For a review of approaches relying on electrophilic amination, see: a) A. Ricci, *Modern Amination Methods*, Wiley-VCH, Weinheim, **2000**; b) T. J. Barker, E. R. Jarvo, *Synthesis* **2011**, 3954 – 3964; c) C. Greck, B. Drouillat, C. Thomassigny, *Eur. J. Org. Chem.* **2004**, 1377 – 1385; d) C. Greck, J. P. Genêt, *Synlett* **1997**, 741 – 748; e) E. Erdik, M. Ay, *Chem. Rev.* **1989**, *89*, 1947 – 1980; f) P. Starkov, T. F. Jamison, I. Marek, *Chem. Eur. J.* **2015**, *21*, 5278 – 5300; for a selection of specific methods, see g) T. J. Barker, E. R. Jarvo, *Angew. Chem. Int. Ed.* **2011**, *50*, 8325 – 8328; *Angew. Chem.* **2011**, *123*, 8475 – 8478; h) P. Dembech, G. Seconi, A. Ricci, *Chem. Eur. J.* **2000**, *6*, 1281 – 1286; i) I. Sapountzis, P. Knochel, *Angew. Chem. Int. Ed.* **2004**, *43*, 897 – 900; *Angew. Chem.* **2004**, *116*, 915 – 918.

[4] Seminal work: a) J.-C. Fiaud, H. B. Kagan, *Tetrahedron Lett.* **1971**, *12*, 1019 – 1022; recent work: b) M. Hatano, K. Yamashita, K. Ishihara, *Org. Lett.* **2015**, *17*, 2412 – 2415; c) J. M. Curto, J. S. Dickstein, S. Berritt, M. C. Kozlowski, *Org. Lett.* **2014**, *16*, 1948 – 1951; d) Y. Mizutani, H. Tanimoto, T. Morimoto, Y. Nishiyama, K. Kakiuchi, *Tetrahedron Lett.* **2012**, *53*, 5903 – 5906; e) M. Hatano, K. Yamashita, M. Mizuno, O. Ito, K. Ishihara, *Angew. Chem. Int. Ed.* **2015**, *54*, 2707 – 2711; *Angew. Chem.* **2015**, *127*, 2745 – 2749; f) J. S. Dickstein, M. W. Fennie, A. L. Norman, B. J. Paulose, M. C. Kozlowski, *J. Am. Chem. Soc.* **2008**, *130*, 15794 – 15795.

[5] For review articles, see: a) J. S. Dickstein, M. C. Kozlowski, *Chem. Soc. Rev.* **2008**, *37*, 1166 – 1173; b) Y. Yamamoto, W. Ito, *Tetrahedron* **1988**, *44*, 5415 – 5423; c) M. Shimizu, *Pure Appl. Chem.* **2006**, *78*, 1867; d) M. Shimizu, I. Hachiya, I. Mizota, *Chem. Commun.* **2009**, 874 – 889; e) S. Hata, M. Shimizu, *J. Synth. Org. Chem. Jpn.* **2011**, *69*, 1134 – 1144.

[6] For cyclopentadieneimines, see: a) R. A. Hagopian, M. J. Therien, J. R. Murdoch, *J. Am. Chem. Soc.* **1984**, *106*, 5753 – 5754; for fluorenylimines, see: b) W. Dai, R. Srinivasan, J. A. Katzenellenbogen, *J. Org. Chem.* **1989**, *54*, 2204 – 2208; for quinone imines, see: c) J. Honzl, M. Metalová, *Tetrahedron* **1969**, *25*, 3641 – 3652; d) J. Brachi, A. Rieker, *Synthesis* **1977**, 708 – 711; for N-heterocycles, see: e) J. J. A. Campbell, S. J. Noyce, R. C. Storr, *J. Chem. Soc. Chem. Commun.* **1983**, 1344 – 1346; f) D. Hunter, D. G. Neilson, *J. Chem. Soc. Perkin Trans. 1* **1984**, 2779 – 2783; g) J. Faragó, Z. Novák, G. Schlosser, A. Csámpai, A. Kotschy, *Tetrahedron* **2004**, *60*, 1991 – 1996; h) S. Tolshchina, G. Rusinov, V. Charushin, *Chem. Heterocycl. Compd.* **2013**, *49*, 66 – 91; i) M. C. Wilkes, *J. Heterocycl. Chem.* **1991**, *28*, 1163 – 1164; j) Q. Zhou, P. Audebert, G. Clavier, F. Miomandre, J. Tang, *RSC Adv.* **2014**, *4*, 7193 – 7195; k) D. Hunter, D. G. Neilson, T. J. R. Weakley, *J. Chem. Soc. Perkin Trans. 1* **1985**, 2709 – 2712; l) A. Ohsawa, T. Kaihoh, H. Igeta, *J. Chem. Soc. Chem. Commun.* **1985**, 1370 – 1371; for bis(imino)pyridines, see: m) I. Khorobkov, S. Gambarotta, G. P. A. Yap, *Organometallics* **2002**, *21*, 3088 – 3090; n) G. K. B. Clentsmith, V. C. Gibson, P. B. Hitchcock, B. S. Kimberley, C. W. Rees, *Chem. Commun.* **2002**, 1498 – 1499.

[7] I. Marek, *Titanium and Zirconium in Organic Synthesis*, Wiley-VCH, Weinheim, **2002**.

[8] For reviews on metallacycle-mediated synthesis, see: a) U. Rosenthal, V. V. Burlakov, M. A. Bach, T. Beweries, *Chem. Soc. Rev.* **2007**, *36*, 719 – 728; b) S. Roy, U. Rosenthal, E. D. Jemmis, *Acc. Chem. Res.* **2014**, *47*, 2917 – 2930; c) H. A. Reichard, G. C. Micalizio, *Chem. Sci.* **2011**, *2*, 573 – 589; d) K. M. Doxsee, J. K. M. Mouser, J. B. Farahi, *Synlett* **1992**, 13 – 21.

[9] a) O. Tomashenko, V. Sokolov, A. Tomashevskiy, A. de Meijere, *Synlett* **2007**, 0652 – 0654; b) O. Tomashenko, V. Sokolov, A. Tomashevskii, A. Potekhin, A. de Meijere, *Russ. J. Org. Chem.* **2007**, *43*, 1421 – 1426; c) R. Wang, B. T. Gregg, W. Zhang, K. C. Golden, J. F. Quinn, P. Cui, D. O. Tymoshenko, *Tetrahedron Lett.* **2009**, *50*, 7070 – 7073; d) O. A. Tomashenko, A. E. Rudenko, V. V. Sokolov, A. A. Tomashevskiy, A. de Meijere, *Eur. J. Org. Chem.* **2010**, 1574 – 1578.

[10] For a (dimeric) solid-state structure of a magnesium ketimide complex, see: K. Manning, E. A. Petch, H. M. M. Shearer, K. Wade, *J. Chem. Soc. Chem. Commun.* **1976**, 107 – 108.

[11] For a review of Group 4 ketimide complexes, see: a) M. J. Ferreira, A. M. Martins, *Coord. Chem. Rev.* **2006**, *250*, 118 – 132; for seminal work on early-transition-metal ketimido complexes, see: b) K. Farmery, M. Kilner, C. Midcalf, *J. Chem. Soc. A* **1970**, 2279 – 2285; c) M. Kilner, C. Midcalf, *J. Chem. Soc. D* **1970**, 552 – 553; d) M. R. Collier, M. F. Lappert, J. McMeeking, *Inorg. Nucl. Chem. Lett.* **1971**, *7*, 689 – 694.

[12] a) J. R. Hagadorn, J. Arnold, *Organometallics* **1998**, *17*, 1355 – 1368; b) D. M. Giolando, K. Kirschbaum, L. J. Graves, U. Bolle, *Inorg. Chem.* **1992**, *31*, 3887 – 3890.

[13] a) F. Loose, I. Plettenberg, D. Haase, W. Saak, M. Schmidtmann, A. Schäfer, T. Müller, R. Beckhaus, *Organometallics* **2014**, *33*, 6785 – 6795; b) D. Thomas, W. Baumann, A. Spannenberg, R. Kempe, U. Rosenthal, *Organometallics* **1998**, *17*, 2096 – 2102.

[14] a) L. D. Durfee, I. P. Rothwell, *Chem. Rev.* **1988**, *88*, 1059 – 1079; Group 4: b) S. L. Buchwald, M. W. Wannamaker, B. T. Watson, *J. Am. Chem. Soc.* **1989**, *111*, 776 – 777; c) S. L. Buchwald, B. T. Watson, M. W. Wannamaker, J. C. Dewan, *J. Am. Chem. Soc.* **1989**, *111*, 4486 – 4494; d) R. B. Grossman, W. M. Davis, S. L. Buchwald, *J. Am. Chem. Soc.* **1991**, *113*, 2321 – 2322; e) M. C. J. Harris, R. J. Whitby, J. Blagg, *Tetrahedron Lett.* **1995**, *36*, 4287 – 4290; see also refs. [7, 16, 17, 19]; for Group 5, see: f) J. M. P. Lauzon, L. L. Schafer, *Dalton Trans.* **2012**, *41*, 11539 – 11550; g) E. Chong, P. Garcia, L. L. Schafer, *Synthesis* **2014**, *46*, 2884 – 2896; h) A. L. Reznichenko, K. C. Hultzsch, *J. Am. Chem. Soc.* **2012**, *134*, 3330 – 3311; i) P. Eisenberger, R. O. Ayinla, J. M. P. Lauzon, L. L. Schafer, *Angew. Chem. Int. Ed.* **2009**, *48*, 8361 – 8365; *Angew. Chem.* **2009**, *121*, 8511 – 8515; j) E. Chong, J. W. Brandt, L. L. Schafer, *J. Am. Chem. Soc.* **2014**, *136*, 10898 – 10901.

[15] a) J. Christoffers, A. Baro, *Quaternary Stereocenters: Challenges and Solutions for Organic Synthesis*, Wiley-VCH, Weinheim, **2005**; b) J. P. Das, I. Marek, *Chem. Commun.* **2011**, *47*, 4593 – 4623; c) J. Christoffers, A. Baro, *Adv. Synth. Catal.* **2005**, *347*, 1473 – 1482; d) I. Denissova, L. Barriault, *Tetrahedron* **2003**, *59*, 10105 – 10146; e) K. Fuji, *Chem. Rev.* **1993**, *93*, 2037 – 2066.

[16] a) F. Sato, S. Okamoto, *Adv. Synth. Catal.* **2001**, *343*, 759 – 784; b) F. Sato, H. Urabe, S. Okamoto, *Chem. Rev.* **2000**, *100*, 2835 – 2886; c) F. Sato, H. Urabe, S. Okamoto, *Synlett* **2000**, 0753 – 0775.

[17] a) M. Takahashi, M. McLaughlin, G. C. Micalizio, *Angew. Chem. Int. Ed.* **2009**, *48*, 3648 – 3652; *Angew. Chem.* **2009**, *121*, 3702 – 3706; b) M. A. Tarselli, G. C. Micalizio, *Org. Lett.* **2009**, *11*, 4596 – 4599; c) M. Z. Chen, M. McLaughlin, M. Takahashi, M. A. Tarselli, D. Yang, S. Umemura, G. C. Micalizio, *J. Org. Chem.* **2010**, *75*, 8048 – 8059; d) D. Yang, J. Belardi, G. C. Micalizio, *Tetrahedron Lett.* **2011**, *52*, 2144 – 2147; e) I. L. Lysenko, H. G. Lee, J. K. Cha, *Org. Lett.* **2009**, *11*, 3132 – 3134; for a brief rationalization of the observed selectivities, see the Supporting Information; for examples with allenic alcohols, see ref. [19].

[18] Similarly, Micalizio et al. observed an erosion of optical purity in the enantioselective allylic alcohol–imine coupling when examining allylic alcohols without terminal substitution of the alkene, see ref. [17].

[19] For examples demonstrating the use of allenic alcohols in carbometalation and formal metallo-[3,3]-rearrangments, see: a) H. L. Shimp, G. C. Micalizio, *Chem. Commun.* **2007**, 4531 – 4533; b) M. McLaughlin, H. L. Shimp, R. Navarro, G. C. Micalizio, *Synlett* **2008**, 735 – 738; c) H. L. Shimp, A. Hare, M. McLaughlin, G. C. Micalizio, *Tetrahedron* **2008**, *64*, 3437 – 3445. See also ref. [16b].

[20] The construction of nitrogen – aryl bonds is of particular interest, see: S. D. Roughley, A. M. Jordan, *J. Med. Chem.* **2011**, *54*, 3451 – 3479.

[21] Y. Wang, W. Yang, H. J. Finlay, L. S. Harikrishnan, J. Jiang, M. G. Kamau, K. Van Kirk, D. S. Nirschl, D. S. Taylor, A. Y. A. Chen, X. Yin, P. G. Sleph, R. Z. Yang, C. S. Huang, L. P. Adam, R. M. Lawrence, R. R. Wexler, M. E. Salvati, *Bioorg. Med. Chem. Lett.* **2014**, *24*, 860 – 864.

[22] In particular, the 1,2-addition of organometallic reagents to imines is a challenging transformation due to the innate low reactivity of the substrate and generally requires activating groups; for recent reports, see: a) A. Desmarchelier, P. Ortiz, S. R. Harutyunyan, *Chem. Commun.* **2015**, *51*, 703 – 706; b) R. Reingruber, S. Bräse, *Chem. Commun.* **2008**, 105 – 107; see also ref. [1].

Received: September 17, 2015
Published online on November 6, 2015

